

Fabrication and Characterization of a Nanowire/Polymer-Based Nanocomposite for a Prototype Thermoelectric Device

Alexis R. Abramson, *Member, ASME*, Woo Chul Kim, *Member, ASME*, Scott T. Huxtable, *Member, ASME*, Haoquan Yan, Yiyang Wu, Arun Majumdar, *Fellow, ASME*, Chang-Lin Tien, *Fellow, ASME*, and Peidong Yang

Abstract—This paper discusses the design, fabrication and testing of a novel thermoelectric device comprised of arrays of silicon nanowires embedded in a polymer matrix. By exploiting the low-thermal conductivity of the composite and presumably high-power factor of the nanowires, a thermoelectric figure of merit, higher than the corresponding bulk value, should result. Arrays were first synthesized using a vapor-liquid-solid (VLS) process leading to one-dimensional (1-D) growth of single-crystalline nanowires. To provide structural support while maintaining thermal isolation between nanowires, parylene, a low thermal conductivity and extremely conformal polymer, was embedded within the arrays. Mechanical polishing and oxygen plasma etching techniques were used to expose the nanowire tips and a metal contact was deposited on the top surface. Scanning electron micrographs (SEMs) illustrate the results of the fabrication processes. Using a modification of the 3ω technique, the effective thermal conductivity of the nanowire matrix was measured and 1 V characteristics were also demonstrated. An assessment of the suitability of this nanocomposite for high thermoelectric performance devices is given. [1016]

Index Terms—Composite, nanowires, thermal conductivity, thermoelectric device.

I. INTRODUCTION

OVER the past decade, considerable research efforts have focused on understanding and manipulating thermal transport in micro/nanostructures. Although results have benefited many technologies, promising research has prompted renewed interest in thermoelectric devices. In particular, considerable attention has been paid to fabricating micro/nanostructures that, due to their reduced dimensionality, exhibit desirable thermoelectric properties including low thermal conductivity and enhanced thermopower. For a

thermoelectric cooler to be comparable in efficiency to the standard vapor-compression cycle refrigerator, the dimensionless thermoelectric figure of merit, ZT , which is a measure of the performance of the material, must be higher than ~ 3.0 at room temperature [1]. The formulation for ZT is given as

$$ZT = \frac{\sigma S^2 T}{k} \quad (1)$$

where S is the Seebeck coefficient, T is absolute temperature, and σ and k are the electrical and thermal conductivity, respectively. Much of the research in this area has investigated the use of superlattices, two-dimensional (2-D) structures consisting of alternating layers of thin films, which impede heat flow in the cross-plane direction. Many promising experimental discoveries have reported dimensionless figures of merit of approximately 1.0, with the most recent unmatched claim of 2.4 in $\text{Bi}_2\text{Te}_3/\text{Sb}_2\text{Te}_3$ superlattices [2].

Even though superlattices hold promise as good thermoelectric materials, theoretically a device composed of nanowires may provide a superior alternative. In certain nanowire systems, the one-dimensionality of the structures may result in confinement of the charge carriers and phonons, thereby affecting transport characteristics, and consequently leading to an enhanced thermoelectric figure of merit [3]–[7]. More specifically, quantum confinement of electrons in nanowires allows tailoring of the electronic band structure. Boundary scattering (which may dominate phonon interaction) and phonon confinement (which influences the phonon spectra and lifetime [8]) can lead to a further reduction in the thermal conductivity. Khitun *et al.* [9] also demonstrated theoretically that an increase in the thermoelectric figure of merit was expected for quantum wires embedded within a matrix of distinctly different acoustic properties. Results of thermal transport in nanowires or nanowire arrays are becoming more prevalent in the literature, but there is still limited experimental evidence of the unusual physical phenomena that arise at this length scale. Nonetheless, experimental investigations have included measurements of the thermal conductivity of individual GaAs nanowires [10], silicon-nitride nanowires [11] and doped and undoped silicon nanowires [12].

To facilitate the incorporation of a thermoelectric device composed of nanowires into real technologies where a consequential amount of thermal energy transfer is required, mesoscale nanowire arrays could be used. The appropriately doped parallel nanowires could be grown perpendicular to a substrate sur-

Manuscript received March 10, 2003; revised December 10, 2003. This work was supported by the National Science Foundation, Nanoscale Interdisciplinary Research Team Grant Program. Subject Editor H. Fujita.

A. R. Abramson is with the Mechanical and Aerospace Engineering Department, Case Western Reserve University, Cleveland, OH 44106-7222 USA (e-mail: alexis.abramson@case.edu).

W. C. Kim and A. Majumdar are with the Department of Mechanical Engineering, University of California, Berkeley, CA 94720-1740 USA.

S. T. Huxtable is with the Department of Mechanical Engineering, Virginia Tech, Blacksburg, VA 24061 USA.

H. Yan and P. Yang are with the Department of Chemistry, University of California, Berkeley, CA 94720-1460 USA.

Y. Wu is with the Department of Chemistry and Biochemistry, University of California, Santa Barbara, CA 93106-9510 USA.

C.-L. Tien, deceased, was with the Department of Mechanical Engineering, University of California, Berkeley, CA 94720-1740 USA.

Digital Object Identifier 10.1109/JMEMS.2004.828742

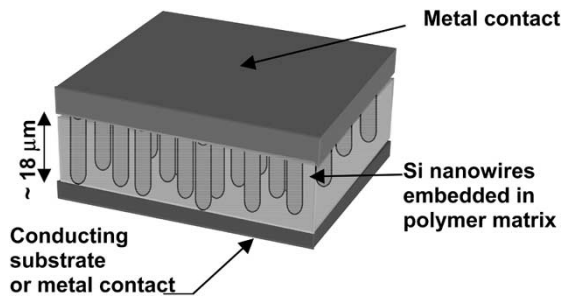


Fig. 1. Schematic diagram of a thermoelectric device component.

face and should individually exhibit good thermoelectric properties. The approach of using nanowire arrays in thermoelectric devices has been theoretically proposed by various researchers [13]–[17]. However, the fabrication complexities and properties of an actual working device are difficult to predict in advance. This study reports on a prototype design of a silicon nanowire array embedded in a polymer matrix to be used as a thermoelectric device component. Fig. 1 shows a schematic of the design. If a conducting semiconductor substrate, complimentary in type to the nanowires (n-type if the nanowires are p-type and vice versa) were used, then the substrate could serve as the counterpart material to form the thermoelectric device. However for the best achievable performance, the component (as shown in Fig. 1) could be fabricated to consist of either n- or p-type Si nanowires that when combined with its p- or n-type counterpart would form a single device. A cascade of these devices electrically in series and thermally in parallel provide additional cooling/power capabilities. In this paper, various fabrication steps are outlined and property measurements are given to provide future direction for any necessary improvements to the device.

II. FABRICATION OF THERMOELECTRIC DEVICE COMPONENT

A. Nanowire Growth

Several techniques to synthesize nanowires and nanotubes have been attempted recently [17]–[24]. One promising and relatively simple method takes advantage of the vapor-liquid-solid (VLS) growth mechanism that was first proposed in the 1960s for large whisker growth [25]. This technique is particularly attractive because single-crystalline nanowires comprised of a wide range of materials can be synthesized with control of doping, diameter and growth orientation. Through careful control of growth conditions, nanowire morphologies such as Si/SiGe superlattice nanowires can also be synthesized, which may be potentially valuable for thermoelectric applications. For this work, doped silicon nanowire arrays were synthesized using the VLS technique, leading to one-dimensional (1-D) growth of single-crystalline vertical nanowires [24]. As shown schematically in Fig. 2, a Si (111) wafer coated with a thin layer of Au was used for growth of an Si nanowire array. Upon thermal annealing, the Au layer formed a liquid alloy with the underlying Si, and due to surface tension effects, produced nanoscale liquid droplets. A gas mixture of SiCl_4 and H_2 was then introduced and preferentially deposited into the Au-Si alloy droplet. After becoming supersaturated within the alloy,

solid Si precipitated out, pushing up the solid/liquid interface and growing the Si nanowires. Each wire formed with an alloy droplet solidified on the nanowire tip. One-dimensional growth proceeded as long as the nanodroplet remained liquid and there was ample reactant gas available [26]. The epitaxial relationship between the Si nanowires and the underlying Si (111) wafer resulted in a vertically oriented array of Si nanowires that typically grew in the direction along the $\langle 111 \rangle$ axis. The diameter of the nanowire was only slightly larger than the size of the original nanodroplets, which was determined by pressure and temperature conditions [27], and the nanowire diameter generally varied by $\pm 10\%$ across the entire array. The nanowires were doped by flowing an additional doping gas during the process. Fig. 3 shows an SEM image of a boron-doped Si nanowire array on a Si (111) substrate. The bright spots in the picture are due to the formation of the alloy droplet at the tip. The doped Si nanowires used for the prototype thermoelectric device were approximately 200 nm in diameter and 18 μm in height. The density of vertical Si nanowires ranged from 10 to 50 million nanowires per cm^2 or center-to-center spacings of approximately 5–7 diameters. This is equivalent to a nanowire filling factor of less than 2%.

B. Nanocomposite Material

The fabrication of the nanowire composite matrix commanded the consideration of a variety of design factors. First, the main purpose of the composite material to be embedded among the nanowires was to provide structural stability to the array. The Si nanowires were extremely fragile; swabbing the surface of the structure would destroy the array, and a slip of the tweezers would inflict a scratch that appeared to damage the nanowires in its vicinity. Therefore, the chosen material would have to be deposited in such a manner that it filled in a large fraction of the space between the high aspect ratio nanowires. The second device requirement was to ensure that the chosen material possessed a low-thermal conductivity, preferably one or more orders of magnitude lower than that of Si. This would maintain an overall low thermal conductivity of the nanowire composite, a criterion essential for superior thermoelectric device performance. Third, since the device fabrication requires that contacts be deposited on at least the top surface, the chosen material must be compatible with standard microfabrication processes (e.g., a chemical resistance to standard lithography chemicals), and particularly must be able to withstand a high processing temperature of at least 200 $^\circ\text{C}$. Thermal evaporation of a contact metal onto the surface would be possible at temperatures of approximately this magnitude. Finally, if a film consisting of the matrix material formed on the top surface, the material would have to be etched away using a compatible processing technique to expose the tips of the nanowires prior to the deposition of the metal contact layer.

A variety of materials were tested for the nanowire array composite. Polymers including polyimide and polystyrene were first tried as potential embedding materials using a liquid spin-on process. However, the polymers were too viscous to penetrate the high aspect ratio gaps between nanowires. Consequently, liquid monomer solutions, including both an ultra-violet light cured and anaerobically cured methacrylate

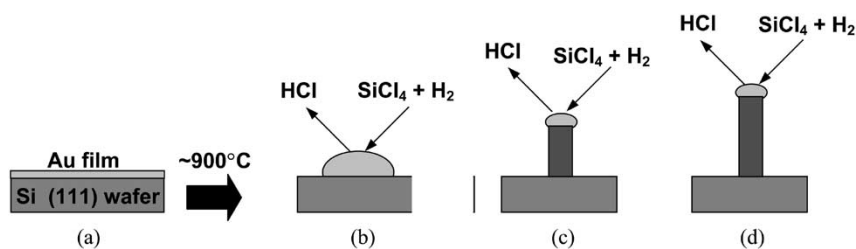


Fig. 2. Schematic diagram of Si nanowire growth by the vapor-liquid-solid (VLS) method: (a) gold film on an Si substrate prior to thermal annealing; (b) nanodroplet is exposed to a silane (SiCl₄) and H₂ gas mixture; SiCl₄ is reduced by H₂ and forms Si; the gold forms an alloy with Si and liquefies; (c) when the liquid is supersaturated, the Si precipitates out and crystallizes the nanowires; (d) further condensation and dissolution of Si increases the length of the nanowire.

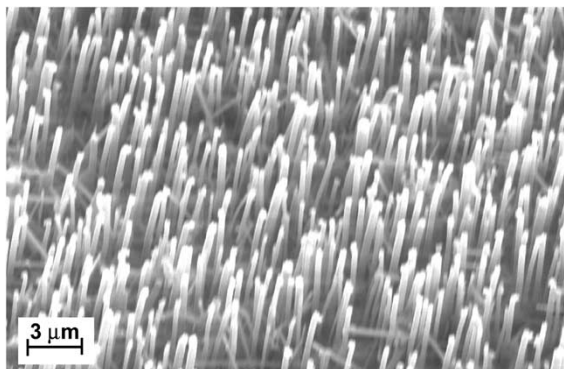
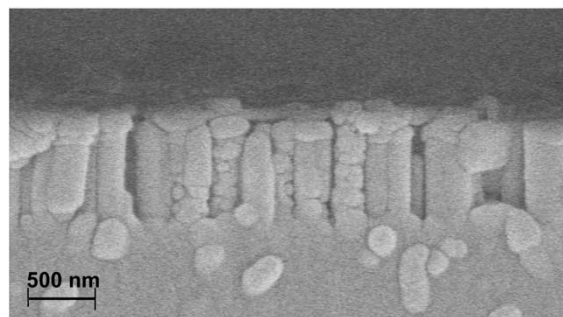
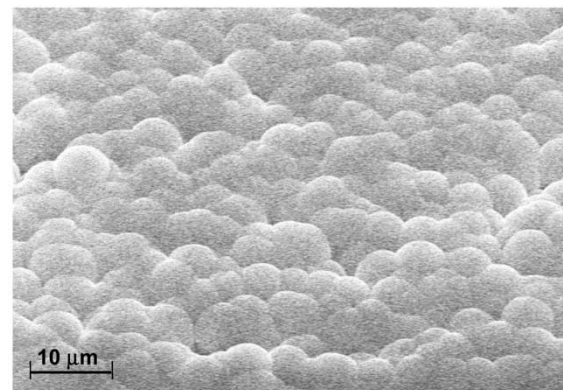


Fig. 3. SEM image of a boron-doped Si nanowire array.

solution, were tested, although cracking upon curing seemed to inhibit structural integrity. Furthermore, controlling the height of the film above the nanowires proved difficult. Parylene N (poly-para-xylylene), a vapor-deposited low thermal conductivity and extremely conformal polymer, was chosen due to its ability to adequately fill the nanowire array and its compatibility with certain lithographic processes. The deposition was achieved in a Specialty Coating Systems Model PDS 2010 LABCOTER 2 system using the manufacturer’s recommended techniques. Maintaining a slight vacuum (0.1–1.0 torr) throughout the process, the dimer, di-para-xylylene, in solid powder form was initially vaporized at ~135 °C. The material then underwent pyrolysis at ~650 °C, breaking into monomer form, and depositing onto the sample maintained at room temperature. Immersing the sample in an adhesion promoter (vinyl trichlorosilane) in an isopropyl alcohol solvent prior to the parylene deposition provided excellent adhesion properties. Scanning electron microscopy (SEM) and focused ion beam (FIB) etching were performed to examine the cross-section and top views of the embedded array. Fig. 4(a) shows an SEM image of a cross-section of a nanowire array partially embedded with parylene (the processing was stopped half-way through processing). The material preferentially deposited on the surface of the nanowire, providing a uniform coating, and continued to grow outward. The nanowires in the figure have diameters of ~100 nm, but during deposition, the parylene engulfed multiple wires together until a relatively uniform composite formed. Fig. 4(b) illustrates the top surface of the nanowire array composite after parylene deposition. The parylene coated the tips of the nanowires during processing, resulting in an undulating top surface. Controlling the parylene



(a)



(b)

Fig. 4. (a) Cross section of a nanowire array partially filled with parylene. (b) Top view (tilted 40°) of a completely filled parylene nanowire array.

deposition process to inhibit formation of a surface parylene film was not feasible.

C. Top Contact Layer

For the thermoelectric device, a metal contact layer must be deposited on the surface of the composite, but the nanowire tips must first be exposed to provide electrical contact. Therefore, following the parylene deposition, an oxygen plasma etching technique was employed to expose the tips of nanowire array. The plasma etch proceeded at a rate of approximately 0.05 μm/min; and using knowledge obtained from SEM images of the height of the array before and after parylene deposition, an approximate processing time was determined to expose the nanowires. In Fig. 5, the tips are clearly shown as bright dots in the SEM image taken following the etching procedure.

To reduce the electrical resistance between the nanowire tip and the top metal contact, the native oxide present on

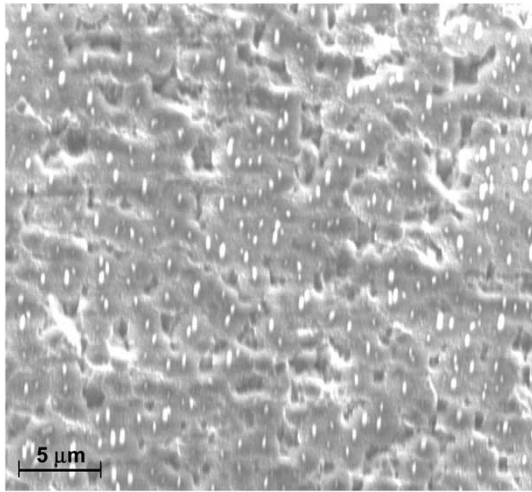


Fig. 5. SEM top view of a Si nanowire array filled with parylene with the top surface etched away to expose the nanowire tips. The gold alloys on the tips appear as bright dots.

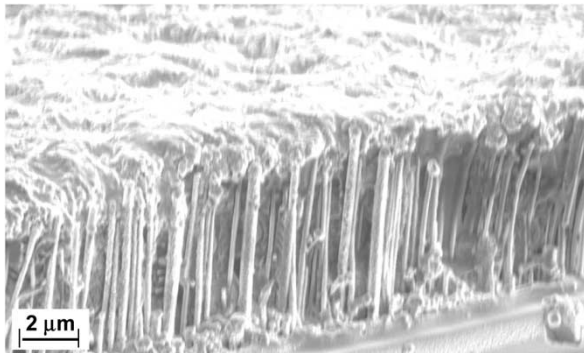


Fig. 6. SEM side view of an Si/parylene nanowire composite following the etching procedure and after a metal layer was deposited on the surface.

the nanowire surface was removed. This was accomplished by dipping the sample in hydrofluoric acid (HF) for two minutes. Since parylene is resistant to HF, only the oxide on the nanowires was affected. After exposing the sample to a nitrogen environment, a chromium/gold contact layer was deposited on the surface using thermal evaporation. Chromium was used as the adhesion layer, and gold was chosen to provide good contact with the alloyed nanowire tips. A side view of the composite plus contact layer is shown in the SEM in Fig. 6. Note that the outer rows of the nanowire array appear to be unfilled with parylene since the exposed parylene on all sides was depleted during the oxygen plasma etch. The gold surface appears to exhibit a high degree of roughness because the conformal polymer left a rough surface upon deposition, which was somewhat maintained even after the oxygen plasma etching procedure. Preliminary tests revealed that the structure adequately conducted electricity from the top metal surface, through the nanocomposite, to the conducting Si substrate.

D. Bottom Contact Layer

A device component comprised of p-doped nanowires and an n-doped substrate should demonstrate thermoelectric properties without the requirement for a complimentary n-doped nanowire component. Nonetheless, a cascade of n-doped and p-doped

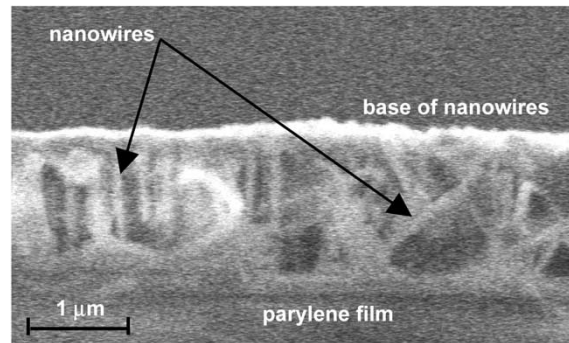


Fig. 7. SEM picture of the nanowire composite + surface parylene film with substrate removed.

nanowire arrays solely connected via metal contact layers, may prove to be a superior design. Therefore, the use of a bottom metal contact layer in place of the substrate was considered. Since the growth of the nanowires can proceed only on a substrate of similar characteristics, it would have to be removed after the nanowire growth process and the deposition of the parylene. This was accomplished by shining a laser of an appropriate transparent wavelength through the bottom of the sample to dissociate and/or melt the nanowire and parylene from the interface. The initial attempt was achieved using a ZnO nanowire array on a sapphire substrate. The array was first filled with parylene until a 2–3 μm surface film formed. Then, a KrF excimer pulsed laser (248 nm) shot at the bottom of the sample at 720 mJ/cm^2 popped the substrate off easily to expose a “tape” of the nanowire composite. An SEM picture of a cross section of the resulting sample is shown in Fig. 7. The base of the nanowire array appears to be relatively intact. The dark spaces may indicate an absence of parylene in the first few layers that resulted after the sample was cut using a diamond saw to obtain a cross section. Following this procedure, the deposition of a metal contact layer could be easily achieved. After further device refinements are made, this technique may be explored further to evaluate its necessity and to determine the feasibility of performing the process on a Si substrate.

III. CHARACTERIZATION OF NANOCOMPOSITE

To characterize the nanocomposite to be used as a thermoelectric device component, current–voltage I – V characteristics were obtained using a two-point probe method. Additionally, the 3ω technique was used to measure the thermal conductivity of the nanocomposite [28]–[30]. This method is particularly suitable for measurement of films and requires the deposition of a metal line, which acts as both a heater and thermometer, on the sample surface. The metal heater/thermometer can be fabricated using standard lithography techniques and a suitable metal deposition process. The general procedure for this method follows by passing a current with angular frequency ω through the heater, which, by Joule heating at a frequency 2ω , heats the surface of the sample. Over a given temperature range, the resistance of the chosen metal increases linearly with increasing temperature; therefore, the electrical resistance of the heater also oscillates at the second harmonic. This 2ω component of the resistance multiplied by the original driving current at ω produces

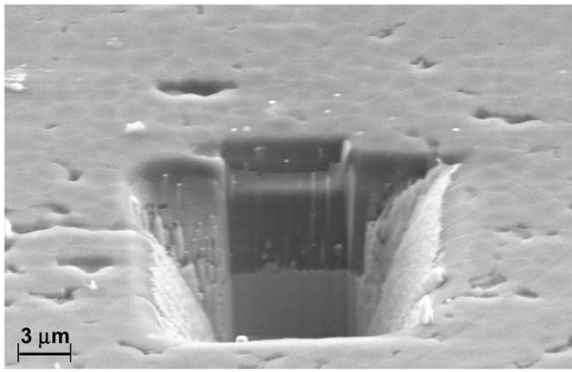


Fig. 8. Using a FIB technique, a hole was etched away from the Si/parylene composite following a mechanical polishing process. The top surface is considerably smoother after polishing. The nanowire tips are seen as bright spots.

a small voltage oscillation at 3ω that can be measured using a lock-in amplifier and can be used to determine the thermal response of the sample [28]–[30]. For a conducting sample, a thin insulating film must be deposited prior to the metal line to provide electrical isolation. From an analysis of the energy transport in the system, and with knowledge of properties of the insulating film and substrate, the thermal conductivity of the sample may be calculated [28]–[30].

A. Sample Fabrication for Measurement

To obtain I – V characteristics of the nanocomposite, two metal pads of $0.1\ \mu\text{m}$ thick Au on $0.04\text{-}\mu\text{m}$ -thick Cr, each $1.2\ \text{mm} \times 1.2\ \text{mm}$ were deposited on the surface of a nanocomposite with exposed nanowire tips [31]. The fabrication methods employed were similar to those of the prototype device to expose the nanowire tips and deposit the two metal pads. A two-point probe method was then used to measure current versus voltage.

For the thermal conductivity measurement, a nanowire composite, different from the one used for the prototype design, was fabricated such that during the parylene deposition, an additional $\sim 2\ \mu\text{m}$ insulating layer of parylene was grown above the height of the nanowires. The approximate thickness of the layer was confirmed by examining SEM pictures both before and after parylene deposition. Regrettably, the micron scale roughness of the parylene film inhibited the deposition of a cohesive metal heater/thermometer able to conduct electricity well. Consequently, a mechanical polishing process was used to reduce the roughness. A synthetic rayon polishing cloth (Buehler Corporation) suitable for polishing polymers along with a $0.05\ \mu\text{m}$ colloidal silica particle size polishing suspension (Buehler Corporation) were used on a mechanical polishing wheel to smooth the sample surface. The procedure took approximately 4 hours to reduce the surface roughness to an average of $35\text{--}50\ \text{nm}$. An FIB technique was used to better examine the cross-section and the top surface of an array embedded with parylene following the mechanical polishing process. A resulting image is shown in Fig. 8. The top surface is noticeably smooth as compared to Fig. 4. Some of the nanowires are visible in the cross-section of the nanocomposite, and the nanowire tips are seen as bright spots. Deposition of the aluminum heater/thermometer line was

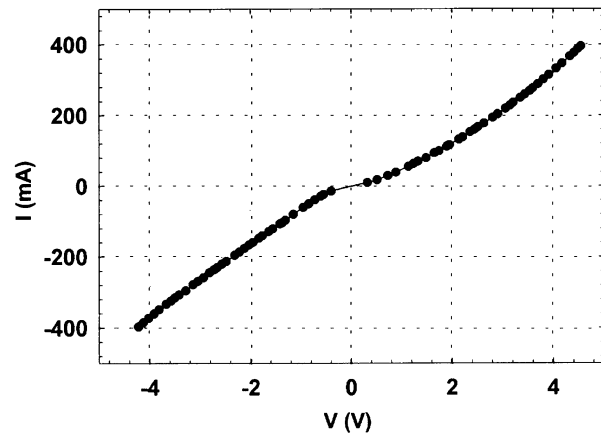


Fig. 9. I – V characteristics of an Si nanowire array embedded with parylene; nanowire tips are exposed. The I – V curve suggests ohmic contact at the junction.

then accomplished using standard lithography techniques and metal evaporation [32], [33]. Specific details of the heater/thermometer fabrication are given elsewhere [32].

B. Results

1) *I – V Characteristics:* The I – V characteristics of the silicon-parylene nanocomposite on an Si substrate were measured and are shown in Fig. 9. The I – V curve indicates that the metal/silicon contact is ohmic. Ohmic contact at the thermoelectric junction ensures that current flow is not obstructed in the device. Furthermore, the I – V curve demonstrates that the boron-doped Si nanowires themselves are conducting as has been shown by others [34], [35]. The nonlinearity near the origin develops into a straight line at high current values, which is a typical I – V characteristic of a heavily doped semiconductor such as the nanowires discussed herein. This behavior occurs because the depletion layer becomes thin with high doping, and electron transport across the junction is dominated by field emission. Specific electrical characteristics such as resistivity of the nanocomposite could not be obtained because the Si substrate on which the nanocomposite was fabricated was also electrically conducting, and therefore the electrical characteristics of the nanocomposite itself could not be isolated. Future experiments that circumvent this problem are ongoing.

2) *Thermal Conductivity of Parylene:* The 3ω technique was first employed in this study to measure the thermal conductivity of a $3\text{-}\mu\text{m}$ parylene film on an Si substrate. Since the parylene film is thinner than the thermal penetration depth and also the heater width, the heat flow through the film is effectively one-dimensional. As a result, temperature oscillations at the interface between the parylene film and Si substrate then penetrate into the semi-infinite substrate. The film simply adds an additional thermal resistance independent of frequency. As described in many [28]–[30], a plot of the amplitude of the temperature oscillations, ΔT (determined from the voltage and resistance measurements) versus $\ln(\omega)$ provides information concerning the thermal conductivity of the substrate. To determine the thermal conductivity of the film, two measurements of the total temperature oscillations can be made, one with the film present and one with the heater

directly on the substrate. The difference between the frequency independent ΔT measurements is the temperature amplitude corresponding only to the film, ΔT_{film} . Then, one-dimensional Fourier law may be applied such that

$$k_{\text{film},y} = \frac{P}{lw} \frac{t_{\text{film}}}{\Delta T_{\text{film}}} \quad (2)$$

where $k_{\text{film},y}$ corresponds to the thermal conductivity of the film in the cross-plane direction, P is the power applied across the metal line, t_{film} is the film thickness, and l and w are the length and the width of the metal line, respectively. Using the temperature rise due solely to the film and assuming isotropic properties, the thermal conductivity of the 3- μm parylene-only film was $\sim 0.12 \pm 0.05$ W/m-K (at room temperature), which compared favorably with the value provided by the manufacturer of the parylene system (Specialty Coating Systems) of ~ 0.125 W/m-K.

3) *Thermal Conductivity of Nanocomposite*: At room temperature, a lock-in amplifier was used to generate the heating current and to measure the third harmonic of the voltage across the metal line as required by the 3ω technique. The data used for the 3ω analysis to extract the thermal conductivity of the nanowire composite were chosen to be within heating frequencies that allowed the thermal wave to penetrate through the top parylene insulating film but not through the entire nanowire composite. In other words, the nanocomposite appeared semi-infinite to the penetrating thermal wave such that $t_{\text{nanocomposite}} \gg \lambda_{\text{pen}} \gg w$, where λ_{pen} is the thermal penetration depth. Therefore, the silicon wafer on which the nanocomposite was grown was not involved in the analysis. The frequency range also guaranteed that 1-D heat flow through the top insulating parylene film was maintained. The general 3ω ‘‘slope method’’ [28] provides for the calculation of the thermal conductivity of a similar semi-infinite medium (i.e., the nanocomposite) from the slope of a plot of the amplitude of the in-phase temperature oscillations, ΔT , versus the natural logarithm of the frequency, $\ln(\omega)$, provided that the sample is isotropic. However, for this study since the thermal conductivity of the nanocomposite film would obviously be quite different in the cross- and in-plane directions, the value calculated using this method would not necessarily provide any interesting information. Therefore, a modified version of the 3ω slope method could be used to account for anisotropy [36]. This analysis demonstrated that the *effective* thermal conductivity determined using the general 3ω slope method could be set equal to the square root of the product of the in- and cross-plane thermal conductivities (k_x and k_y , respectively) such that $k_{\text{eff}} = \sqrt{k_x k_y}$.

The case of a film on substrate was discussed previously for the thermal conductivity measurement of parylene on silicon. A similar approach was taken for the measurement involving the insulating parylene film on the semi-infinite nanocomposite. The parylene film simply adds a frequency independent ΔT to the analysis. With knowledge of the thermal conductivity and thickness of the surface parylene thin film (values of 0.125 W/m-K and 2 μm were used), ΔT_{film} was calculated and subtracted from the total ΔT to give $\Delta T_{\text{nanocomposite}}$. Nonetheless, since the nanocomposite is treated as the semi-infinite medium,

the value for the effective thermal conductivity was calculated from

$$k_{\text{eff}} = \sqrt{k_x k_y} = \frac{V_{1\omega}^3}{4\pi l R^2} \frac{\ln\left(\frac{f_2}{f_1}\right)}{V_{3\omega,1} - V_{3\omega,2}} \frac{dR}{dT} \quad (3)$$

where R is the average resistance of the metal line, dT/dR is the derivative of the $T(R)$ calibration line, $V_{1\omega}$ is the voltage applied to generate the heating current at ω and $V_{3\omega}$ is the voltage measured at the third harmonic, f is the frequency in Hz, and subscripts 1 and 2 on the frequencies and third harmonic voltages represent the measurements at two distinct points along the straight line of the in-phase ΔT versus $\ln(\omega)$ plot. Consequently, a value for the effective thermal conductivity of the nanocomposite was calculated as 0.78 ± 0.16 W/m-K for the room temperature measurement. A series resistance analysis demonstrated that since the nanowire filling factor was less than 2%, then for any reasonable value of the thermal conductivity of the nanowire (10–200 W/m-K), k_x would always be equal to ~ 0.12 W/m-K. Using $k_{\text{eff}} = \sqrt{k_x k_y}$ from (3), then $k_y \approx 4.9 \pm 2.2$ W/m-K.

Since thermal conduction through the nanocomposite in the cross-plane direction follows paths through both silicon and parylene, treating these paths as parallel resistances offers the opportunity for an interesting comparison with the results obtained from the 3ω technique. From an extrapolation of thermal conductivity data gained from experiments on similar individual Si nanowires presented by Li *et al.* [12] and using the thermal conductivity of parylene as described above, a predicted value for k_y of the nanocomposite was estimated by performing a parallel thermal resistance calculation. Using a value of $k_{\text{nanowire}} = 60$ W/m-K and $k_{\text{parylene}} = 0.12$ W/m-K, then $k_y = 1.3$ W/m-K. Although lower than the measured value of 4.9 W/m-K, the order of magnitude is comparable.

4) *Figure of Merit Approximation*: While a measurement for the Seebeck coefficient or electrical conductivity could not be performed on the nanocomposite, generally the thermopower, $S^2\sigma$ can be enhanced in low-dimensional structures such as nanowires [3]–[7]. The question remains as to whether the enhancement may be realized in these nanowires or whether smaller diameter and/or different materials may be required. Nonetheless, using the value for the resistivity for a similar boron-doped Si nanowire given by Cui *et al.* [35], 6.9×10^{-3} $\Omega\text{-cm}$ and assuming a fill factor of 2% and parylene resistivity of 1.4×10^{17} $\Omega\text{-cm}$ (Specialty Coating Systems), it is apparent that the parylene acts as an electrical insulator and that the path of electrical conduction is through the nanowires. Therefore, the electrical conductivity, the inverse of the total resistivity of the nanocomposite, may be approximated as 2.9 S/cm. Without assuming any enhancement to the Seebeck coefficient due to the reduced dimensionality of Si, and using a published value of 450 $\mu\text{V/K}$ [37], an approximation for the dimensionless figure of merit (at room temperature) was calculated as $\sim 3.6 \times 10^{-4}$. A more rigorous analytical approach [38] was also used to determine ZT for the case of a composite comprised of parallel cylinders in a matrix material, and a similar value was calculated. This value is approximately the same order of magnitude as the published value for bulk Si

[37]. Even if the Seebeck coefficient were enhanced beyond the published value, the increase would likely not be high enough to make the Si-based nanocomposite suitable for applications requiring a high thermoelectric performance. Smaller diameter wires and/or better thermoelectric materials must be explored.

IV. CONCLUSION

A novel thermoelectric device using an Si nanowire array embedded in a parylene matrix was designed. The main purpose of this study was to investigate the fabrication of such a device and to use results from its characterization to offer future directions. Fabrication details of the device were discussed and thermal conductivity results and I - V characteristics were presented. Ohmic contact was shown to exist at the metal/Si junction. Several fabrication steps were tested to develop the prototype design and to build the device used to measure the thermal conductivity. Preliminary tests indicate a low thermal conductivity in comparison with bulk values. A calculation to approximate the figure of merit demonstrated that even if an enhancement to the Seebeck coefficient were realized, the increase would likely not be large enough to make the nanocomposite suitable for high thermoelectric performance applications. Smaller diameter wires and/or better thermoelectric materials must be explored. Nonetheless, thermoelectric measurements are currently in progress along with parametric studies to examine how nanowire diameter and fill factor affect the nanocomposite properties.

ACKNOWLEDGMENT

The authors are extremely grateful to Prof. C.-L. Tien for his valuable insight into this research topic and for his contributions made to the science and engineering community. This work is dedicated in his honor.

REFERENCES

- [1] G. Mahan, B. Sales, and J. Sharp, "Thermoelectric materials: New approaches to an old problem," *Phys. Today*, vol. 50, pp. 42–47, 1997.
- [2] R. Venkatasubramanian, E. Siivola, T. Colpitts, and B. O'Quinn, "Thin-film thermoelectric devices with high room-temperature figures of merit," *Nature*, vol. 413, pp. 597–602, 2001.
- [3] S. S. Kubakadd and B. G. Mulimani, "Thermopower enhancement in semiconducting quantum well wires for acoustic phonon scattering," *J. Appl. Phys.*, vol. 58, pp. 3643–3645, 1985.
- [4] L. D. Hicks, T. C. Harman, and M. S. Dresselhaus, "Use of quantum-well superlattices to obtain a high figure of merit from nonconventional thermoelectric materials," *Appl. Phys. Lett.*, vol. 63, pp. 3230–3232, 1993.
- [5] L. D. Hicks and M. S. Dresselhaus, "Thermoelectric figure of merit of a one-dimensional conductor," *Phys. Rev. B*, vol. 47, pp. 16 631–16 634, 1993.
- [6] X. Sun, Z. Zhang, and M. S. Dresselhaus, "Theoretical modeling of thermoelectricity in Bi nanowires," *Appl. Phys. Lett.*, vol. 74, pp. 4005–4007, 1999.
- [7] O. Rabin, Y. M. Lin, and M. S. Dresselhaus, "Anomalously high thermoelectric figure of merit in $\text{Bi}_{1-x}\text{Sb}_x$ nanowires by carrier pocket alignment," *Appl. Phys. Lett.*, vol. 79, pp. 81–83, 2001.
- [8] M. S. Dresselhaus and P. C. Eklund, "Phonons in carbon nanotubes," *Adv. Phys.*, vol. 49, pp. 705–814, 2000.
- [9] A. Khitun, A. Balandin, and K. L. Wang, "Modification of the lattice thermal conductivity in silicon quantum wires due to spatial confinement of acoustic phonons," *Superlattices Microstructures*, vol. 26, pp. 181–193, 1999.

- [10] A. Potts, M. J. Kelly, D. G. Hasko, C. G. Smith, J. R. A. Cleaver, H. Ahmed, J. Singleton, and T. J. B. Janssen, "Thermal transport in free-standing semiconductor fine wires," *Superlattices Microstructures*, vol. 9, pp. 315–318, 1991.
- [11] T. S. Tighe, J. W. Worlock, and M. L. Roukes, *Appl. Phys. Lett.*, vol. 70, pp. 2687–2689, 1997.
- [12] D. Li, Y. Wu, P. Kim, L. Shi, N. P. Yang, and A. Majumdar, "Thermal conductivity of individual silicon nanowires," *Appl. Phys. Lett.*, vol. 83, pp. 2934–2936, 2003.
- [13] Z. Zhang, J. Y. Ying, and M. S. Dresselhaus, "Bismuth quantum-wire arrays fabricated by a vacuum melting and pressure injection process," *J. Mater. Res.*, vol. 13, pp. 1745–1748, 1998.
- [14] M. S. Dresselhaus, G. Dresselhaus, X. Sun, Z. Zhang, S. B. Cronin, and T. Koga, "Low-dimensional thermoelectric materials," *Phys. Solid State*, vol. 41, pp. 679–682, 1999.
- [15] J. Heremans, C. M. Thrush, Y. M. Lin, S. Cronin, Z. Zhang, M. S. Dresselhaus, and J. F. Mansfield, "Bismuth nanowire arrays: Synthesis and galvanomagnetic properties," *Phys. Rev. B*, vol. 61, pp. 2121–2130, 2000.
- [16] Y. M. Lin, X. Sun, and M. S. Dresselhaus, "Theoretical investigation of thermoelectric transport properties of cylindrical Bi nanowires," *Phys. Rev. B*, vol. 62, pp. 4610–4623, 2000.
- [17] A. L. Prieto, M. S. Sander, M. S. Martin-Gonzales, R. Gronsky, T. Sands, and A. M. Stacy, "Electrodeposition of ordered Bi_2Te_3 nanowire arrays," *J. Amer. Chem. Soc.*, vol. 123, pp. 7160–7161, 2001.
- [18] D. S. Bethune, C. H. Kiang, M. S. Devries, G. Gorman, R. Savoy, J. Vazquez, and R. Beyers, "Cobalt-catalyzed growth of carbon nanotubes with single-atomic-layer walls," *Nature*, vol. 363, pp. 605–607, 1993.
- [19] D. T. Colbert, J. Zhang, S. M. McClure, P. Nikolaev, Z. Cheng, J. H. Hafner, D. W. Owens, P. G. Kotula, C. B. Carter, J. H. Weaver, A. G. Rinzier, and R. E. Smalley, "Growth and sintering of fullerene nanotubes," *Science*, vol. 266, pp. 1218–1222, 1993.
- [20] T. J. Trentler, S. C. Goel, K. M. Hickman, A. M. Viano, M. Y. Chiang, A. M. Beatty, P. C. Gibbons, and W. E. Buhro, "Solution-liquid-solid growth of indium phosphide fibers from organometallic precursors: Elucidation of molecular and nonmolecular components of the pathway," *J. Amer. Chem. Soc.*, vol. 119, pp. 2172–2181, 1997.
- [21] A. M. Morales and C. M. Lieber, "A laser ablation method for the synthesis of crystalline semiconductor nanowires," *Science*, vol. 279, pp. 208–210, 1998.
- [22] P. Nikolaev, "Gas-phase catalytic growth of single-walled carbon nanotubes from carbon monoxide," *Chem. Phys. Lett.*, vol. 313, pp. 91–97, 1999.
- [23] J. D. Holmes, K. P. Johnson, R. C. Doty, and B. A. Korgel, "Control of thickness and orientation of solution-grown silicon nanowires," *Science*, vol. 287, pp. 1471–1473, 2000.
- [24] Y. Y. Wu and P. D. Yang, "Direct observation of vapor-liquid-solid nanowire growth," *J. Amer. Chem. Soc.*, vol. 123, pp. 3165–3166, 2001.
- [25] R. S. Wagner and W. C. Ellis, "Vapor-liquid-solid mechanism of single crystal growth," *Appl. Phys. Lett.*, vol. 4, pp. 89–91, 1964.
- [26] J. Hu, T. W. Odom, and C. M. Lieber, "Chemistry and physics in one dimension: Synthesis and properties of nanowires and nanotubes," *Accounts Chem. Res.*, vol. 32, pp. 435–445, 1999.
- [27] Y. Y. Wu, H. Q. Yan, M. Huang, B. Messer, J. H. Song, and P. Yang, "Inorganic semiconductor nanowires: Rational growth, assembly, and novel properties," *Chem.—A Europ. J.*, vol. 8, pp. 1261–1268, 2002.
- [28] D. G. Cahill, "Thermal conductivity measurement from 30 K to 750 K—The 3ω method," *Rev. Scientif. Instrum.*, vol. 61, pp. 802–808, 1990.
- [29] D. G. Cahill, M. Katiyar, and J. R. Abelson, "Thermal conductivity of a -Si:H thin films," *Phys. Rev. B*, vol. 50, pp. 6077–6081, 1994.
- [30] S. M. Lee and D. G. Cahill, "Heat transport in thin dielectric films," *J. Appl. Phys.*, vol. 81, pp. 2590–2595, 1997.
- [31] W. C. Kim, A. R. Abramson, S. T. Huxtable, A. Majumdar, Y. Y. Wu, L. Trahey, P. Yang, A. Stacy, T. D. Sands, and R. Gronsky, "Nanowire arrays for thermoelectric devices," in *Proc. ASME Heat Transfer Division Summer Meeting*, 2003.
- [32] S. T. Huxtable, A. R. Abramson, A. Majumdar, C. L. Tien, C. LaBounty, X. Fan, G. Zeng, J. E. Bowers, A. Shakouri, and E. T. Croke, "Thermal conductivity of Si/SiGe superlattices," in *Proc. ASME Heat Transfer Division IMECE*, vol. 7, 2001, pp. 223–229.
- [33] S. T. Huxtable, A. R. Abramson, C. L. Tien, A. Majumdar, C. LaBounty, X. Fan, G. H. Zeng, J. E. Bowers, A. Shakouri, and E. T. Croke, "Thermal conductivity of Si/SiGe and SiGe/SiGe superlattices," *Appl. Phys. Lett.*, vol. 80, pp. 1737–1739, 2002.
- [34] D. D. Ma, C. S. Lee, and S. T. Lee, "Scanning tunneling microscopy study of boron-doped silicon nanowires," *Appl. Phys. Lett.*, vol. 79, pp. 2468–2470, 2001.

- [35] Y. Cui, X. F. Duan, J. T. Hu, and C. M. Lieber, "Doping and electrical transport in silicon nanowires," *J. Phys. Chem. B*, vol. 104, pp. 5213–5216, 2000.
- [36] T. Borca-Tasciuc, A. R. Kumar, and G. Chen, "Data reduction in 3 omega method for thin-film thermal conductivity determination," *Rev. Scientif. Instrum.*, vol. 72, pp. 2139–2147, 2001.
- [37] A. W. Van Herwaarden, "The seebeck effect in silicon IC's," *Sens. Actuators*, vol. 6, pp. 245–249, 1984.
- [38] D. J. Bergman and L. G. Fel, "Enhancement of thermoelectric power factor in composite thermoelectrics," *J. Appl. Phys.*, vol. 85, pp. 8205–8216, 1999.



Alexis R. Abramson received the B.S. and M.S. degrees from Tufts University, Medford, MA, and the Ph.D. degree in mechanical engineering from the University of California, Berkeley, in 2002.

She is currently the Warren E. Rupp Assistant Professor in Mechanical and Aerospace Engineering at Case Western Reserve University (CWRU), Cleveland, OH, where she also holds a joint appointment in electrical engineering. Her research focus has been in the general area of nanotechnology, spanning from micro/nanoscale radiation effects

during the processing of microelectronics components to understanding and manipulating nanoscale energy transport in materials. She has also been involved in biomimetic research to explore how the natural world has taken advantage of specific nanoscale phenomena. She is the author of a number of publications in her research field.

Dr. Abramson is a Member of the American Society of Mechanical Engineers (ASME).



Woo Chul Kim received the B.S. degree in mechanical engineering from the Yonsei University, Seoul, Korea, in 1998 and the M.S.M.E. degree in mechanical engineering from the Purdue University, West Lafayette, IN, in 2001. He is currently pursuing the Ph.D. degree at the Mechanical Engineering Department at the University of California, Berkeley.

He joined Dr. Majumdar's group in Fall 2001. His research interests include fabrication and characterization of thermoelectric device out of nanowire arrays and thermal conductivity measurement of thin

films using 3w technique.

Mr. Kim is a Member of the American Society of Mechanical Engineers (ASME).



Scott T. Huxtable received the B.S. degree in mechanical engineering from Bucknell University, PA, in 1997 and the M.S. and Ph.D. degrees in mechanical engineering from the University of California at Berkeley in 1999 and 2002, respectively.

In 2003, he joined Virginia Tech, Blacksburg, VA, where he is an Assistant Professor in the Mechanical Engineering Department. Before joining Virginia Tech, he was a Postdoctoral Research Associate in the Materials Science Department at the University of Illinois at Urbana-Champaign for one year. His research interests include nanoscale thermal transport and energy conversion.

Dr. Huxtable is a Member of the American Society of Mechanical Engineers (ASME).



Haoquan Yan received the Bachelor of Science degree from the Chemistry Department at the University of Science and Technology of China in 2000, where he was the recipient of the distinguished *Guo Moruo* scholarship, the highest award given to a student. He is currently pursuing the Ph.D. degree in the Chemistry Department at University of California, Berkeley, where his research topic involves the growth of nanowires for nanolaser and other applications.

He received the Materials Research Society graduate student award at the Fall 2001 meeting for his work on nanowire synthesis.



Yiying Wu received the Ph.D. degree from the Chemistry Department at University of California, Berkeley, in 2002, working with Prof. P. Yang.

He then went to University of California, Santa Barbara, as a Postdoctoral Research with Prof. G. Stucky in the Department of Chemistry and Biochemistry. His research includes controlled syntheses of semiconductor nanowires and the study of single-nanowire electric and thermal properties, mesostructured materials, and confined self-assembly.



Arun Majumdar received the Ph.D. degree in mechanical engineering from the University of California at Berkeley in 1989.

He then served on the Mechanical Engineering faculties at Arizona State University (1989–1992) and the University of California at Santa Barbara (1992–1996). Currently, he holds the Almy and Agnes Maynard Chair in Mechanical Engineering, University of California, Berkeley, where he served as the Vice Chair from 1999 to 2002. His research interests include nanoscale thermophysics, fluidics

and biophysics with applications to energy conversion and biomedical technologies.

Dr. Majumdar is a recipient of the NSF Young Investigator Award, the ASME Melville Medal, ASME Heat Transfer Division Best Paper Award, and 2001 ASME Gustus Larson Memorial Award. He is currently serving as an Editor for the *International Journal of Heat and Mass Transfer* and Co-Editor-in-chief of *Microscale Thermophysical Engineering*. He also serves as Chair, Board of Advisors, ASME Nanotechnology Institute; Member, Council on Materials Science and Engineering, U.S. Department of Energy; and Member, Nanotechnology Technical Advisory Group to the President's Council of Advisors on Science and Technology (PCAST). He is a Fellow of the American Society of Mechanical Engineers (ASME) and AAAS.



Chang-Lin Tien enriched the educational experience of the University of California at Berkeley (UC Berkeley) while strengthening the University's reputation around the globe. An internationally recognized expert in heat transfer processes, he authored or edited more than 300 research publications. The distinction of his work earned him many honors, including the Max Jakob Memorial Award, the highest international award in his field. A committed educator who taught thousands of UC Berkeley students—including more than 60 students

whose doctoral work he directed—Dr. Tien also received the UC Berkeley's Distinguished Teaching Award. As UC Berkeley's Chancellor from 1990 to 1997, Dr. Tien successfully led efforts to develop a more stable funding base for UC Berkeley in the face of declining support. Throughout his academic career, he also lent his inexhaustible vision, drive, and humanity to a wide range of partnerships between the education sector and its colleagues in government, business, and the community, both at home and abroad. Dr. Tien retired from the UC Berkeley in 2001 as University Professor and the NEC Distinguished Professor in the Department of Mechanical Engineering. He was a Fellow of the American Society of Mechanical Engineers (ASME). He died October 29, 2002 at the age of 67.



Peidong Yang received the B.S. degree in chemistry from University of Science and Technology of China in 1993 and the Ph.D. in chemistry from Harvard University, Cambridge, MA, in 1997.

He then was a Postdoctoral Researcher in the area of mesoporous materials at University of California, Santa Barbara. He began his faculty appointment in the Department of Chemistry at the University of California at Berkeley in 1999. He is currently holding the ChevronTexaco Assistant Professorship in Department of Chemistry.